Abbreviations and Acronyms

^{18}FDG = [^{18}F]-fluoro-deoxy-glucose
BDM = 2,3-butanedione-2-monoxime
CDC = cardiac-derived stem cells
CT = computed tomography
FAC = fractional area change
FG = fibrin glue
MI = myocardial infarction
PBS = phosphate-buffered saline
PCR = polymerase chain reaction
PET = positron emission tomography
qPCR = quantitative polymerase chain reaction
WKY = Wistar Kyoto

retention is <10%, after intramyocardial, intracoronary, or retrograde transvenous cell delivery, emphasizing the inefficiency of the currently used methods for intracardiac stem cell transplantation (5). There is a clear need for a noninvasive, accurate, and readily translatable technique for quantification of cell engraftment that would allow rapid assessment of the efficacy of any cell delivery strategy. Within this context, in vivo imaging can play a major role (15,16).

Here we used positron emission tomography (PET) for in vivo quantification of retention of [^{18}F]-fluoro-deoxy-glucose (^{18}FDG) labeled cells after direct intramyocardial delivery, in a rat myocardial infarction (MI) model. We validated the quantitative data derived noninvasively by PET with one of the most sensitive laboratory techniques (qPCR). With PET as a tool, we investigated the role of cardiac contraction and perfusion on cell retention, and we tested various interventions to optimize cell delivery, namely a mechanical plug at the site of injection, and drugs to lower heart rate or to suppress contractility. Sealing the injection site with fibrin glue (FG) and lowering heart rate by adenosine significantly improved cell retention. Importantly, the former intervention translated into a longer-term boost of engraftment and functional improvement in the same model.

Methods

Cells. Cardiac-derived stem cells (CDCs) were cultured from tissue samples derived from explanted hearts from male 3-month-old Wistar Kyoto (WKY) rats (Harlan, Indianapolis, Indiana), as previously described (17,18). The WKY are inbred syngeneic rats and therefore appropriate for use in cell transplantation studies, without the need for immunosuppression (19,20).

In vitro ^{3}H-FDG labeling. The 10^5 cells were incubated in glucose-free medium for 1 h and exposed to 2 μCi/ml of ^{3}H-FDG with or without insulin (0.1 U/ml) for 30 or 60 min. Tracer uptake was measured by beta-counting.

Radiotoxicity of ^{18}FDG. To assess toxicity of ^{18}FDG, 1,000 cells were incubated with 2 μCi /ml of media ^{18}FDG. Similar number of cells in regular media served as controls. Cell viability and proliferation were examined by a WST-8 colorimetric assay (Cell Counting Kit-8, Dojindo Molecular Technologies, Rockville, Maryland), as per the manufacturer's protocol.

Animal model. Female WKY rats (n = 85 total) underwent left thoracotomy under general anesthesia, and MI was produced by permanent ligation of the left anterior descending coronary artery. The CDCs (2 million, suspended in 150 μl of phosphate-buffered saline [PBS]) were injected directly into the myocardium, at 2 sites into the infarct. Subsequently, the chest was closed, and the animals were transported to the PET scanner. Animal care was in accordance to Johns Hopkins University guidelines (details are provided in the Online Appendix).

Cell injections. Two million CDCs were labeled with ^{18}FDG immediately before injection (Table 1). Subsequently, cells were pelleted by centrifugation for removal of labeling media and washed twice in PBS.

To explore the role of cardiac contraction and coronary blood flow on CDC retention, cardiac arrest was induced in 4 animals by IV thiopental injection through the tail vein. After cardiac arrest was confirmed by visual inspection, cells were injected at 2 sites of the left ventricle. Subsequently, the chest was closed, and the animals underwent PET imaging 1 h after the injection.

In 8 animals, (FG group) cells were injected intramyocardially, in 2 sites, within the infarct border zone. While the needle tip was still in situ, 1 or 2 drops of FG (Tisseel VH-Baxter Healthcare Corp., Glendale, California) were applied directly over each injection site, to provide a seal and prevent backwash of the cells. In 8 animals (cells in PBS group), similarly labeled cells were injected without application of FG.

To determine whether transient suppression of myocardial contraction locally at the site of cell injection could improve retention, cells were resuspended in 150 μl of PBS containing 100 μmol/l 2,3-butanedione-2-monoxime (BDM) (Sigma-Aldrich, St. Louis, Missouri), an excitation-contraction uncoupler (21), and then injected in the myocardium of infarcted rats (n = 6).

Table 1 Description of the Study Groups

Experimental Group	n	Protocol of Cell Injection
Cardiac arrest	4	Cells were injected intramyocardially after the induction of cardiac arrest
Lysed cells	2	Cells were lysed with sonication after labeling and before injection
Cells in PBS	8	Cells were suspended in PBS and injected intramyocardially
BDM	6	Cells were suspended in PBS containing 100 μmol/l of BDM to locally suppress contractility at the injection site
FG	8	After intramyocardial cell injection, the epicardial side of the injection site was sealed by FG
Adenosine	4	Intramyocardial delivery of cells was performed during slowing of ventricular rate by IV injection of adenosine (1 mg)
FG + adenosine	8	Cell delivery was performed during IV adenosine injection and subsequently the injection site was sealed epicardially by FG

BDM = 2,3-butanedione-2-monoxime; FG = fibrin glue; FAC = fractional area change; PBS = phosphate-buffered saline.

Because rats have a heart rate of 300 to 400 beats/min (22), we sought to determine whether the slowing of ventricular rate by the IV injection of adenosine (1 mg) immediately before cell delivery would lead to an increase of acute cell retention, by improving the accuracy of the cell injection (n = 4).

Additionally, in 8 animals, IV adenosine was combined with epicardial FG, to investigate any potential synergistic effect of these 2 interventions.

Finally, to investigate whether radioactivity derived from dead cells could confound quantification, 2 million CDCs were radiolabeled and subsequently lysed by sonication. The lysate was then injected intramyocardially at 2 sites of the infarct border zone, in similarly infarcted Wistar Kyoto rats (n = 2).

In vivo imaging. The PET images were acquired on a GE VISTA (GE Healthcare, Piscataway, New Jersey) small animal PET system. Features of this system have been published before (23). Details about the imaging protocol can be found in the Online Appendix.

A static PET acquisition of the syringe containing the labeled cells (5 min) was obtained immediately before cell injection. After cell injection, the same syringe was imaged again (same imaging parameters), to calculate the net injected radioactivity (that corresponds to the exact cell number delivered in every animal).

After the completion of the ^{18}FDG acquisition, a perfusion PET study with ^{13}NH3 (ammonia) was performed for myocardial delineation (Online Appendix).

After the perfusion scan, [^{18}F]-fluoride was injected to facilitate the co-registration of PET and computed tomography (CT) images obtained with the different scanners as previously described (Online Appendix) (13). The use of micro CT for attenuation correction of micro PET images has recently been shown to be the most accurate technique for this purpose and has been applied in integrated PET/CT scanners (24).

Image analysis. All images were analyzed with AMIDE software (Online Appendix) (25).

Quantification of engraftment by real time PCR. Quantitative PCR was performed 1 h after cell injection in 6 animals (cells in PBS group) and in 16 at 21 days after cell injection (8 of the FG and 8 of the cells in PBS group) to validate the results obtained by PET but also to compare medium term engraftment in these groups. We injected cells isolated from male donor WK rats into the myocardium of female recipients and quantified engrafted donor cell numbers, as a function of time, by real-time PCR, with the SRY gene located on the Y chromosome as target (Online Appendix) (4).

Echocardiography. To assess global cardiac function in 39 rats (cells in PBS [n = 11], FG [n = 11], control group where PBS only was injected [n = 9], and control group where FG was applied epicardially after PBS injection (n = 8]), echocardiography was performed with the Vevo 770 system (Visualsonics, Toronto, Canada) on days 2 and 21 after the induction of MI. The fractional area change (%FAC) was measured on the parasternal long-axis view, and changes from baseline (day 2 after MI) are reported.

Histology. In 6 animals (3 of the cells in PBS group and 3 of the FG group) enhanced green fluorescent protein labeled cells were injected to allow detection by immunocytochemistry (Online Appendix).

Statistical analysis. Values are reported as mean ± SD. The Student *t* test was used to compare cell retention rates, engraftment, and ejection fractions, when comparisons were performed between 2 independent groups. The *t* test with the Welch's correction was used when the assumption of equal variances was not satisfied. One-way analysis of variance was used when the groups were 3 or more, and the Dunnett's test was applied for post-hoc comparisons between the baseline group and the intervention groups. A p value <0.05 was chosen for statistical significance.

Results

Radiolabeling of CDCs with ^{18}FDG. Accumulation of ^{3}FDG in CDCs was 2.2 ± 1.3% of the administered dose after 30 min of exposure and did not show any significant change after 60 min or after addition of insulin in the labeling medium (data not shown). With ^{18}FDG for labeling, 2 μCi/ml had no affect on cell viability and proliferation for up to 7 days after labeling (data not shown). On the basis of these findings, radiolabeling CDCs with a dose of 2 μCi/ml of media for 30 min was selected for in vivo experiments.

In vivo PET imaging. Normally perfused myocardium was delineated by ^{13}NH3 perfusion imaging. The infarct region appeared as a large anterolateral perfusion deficit. Injected cells were easily identified as intramyocardial bright spots by PET, localized within the infarct area and infarct border zone (Figs. 1A to 1C). Coregistration with CT was successful in all animals (Figs. 1D to 1F), allowing accurate in vivo quantification of cell retention.

Retention of intramyocardially injected cells. When nonviable (lysed) cells were injected, %ID was 6.4 ± 4.3%, indicating low reuptake of the released radiolabel by the myocardium.

In the animals that received cells resuspended in plain PBS, retention 1 h after injection was 17.8 ± 7.3%, a low retention rate that is in accordance with previous studies that quantified efficiency of cell delivery by ex vivo methods (4,5).

When cells were injected in the arrested heart, retention increased to 75.8 ± 18.3% ($p < 0.01$ vs. cells in PBS). The arrested heart does not contract or sustain perfusion. Thus, cardiac contraction and/or coronary perfusion are major potential culprits in the early washout of cells from the injection site.

One way that contraction might affect cell retention is by active extrusion of the injectate during each heartbeat. We tested this notion by creating a mechanical plug with FG at

JACC Vol. 54, No. 17, 2009
October 20, 2009:1619–26

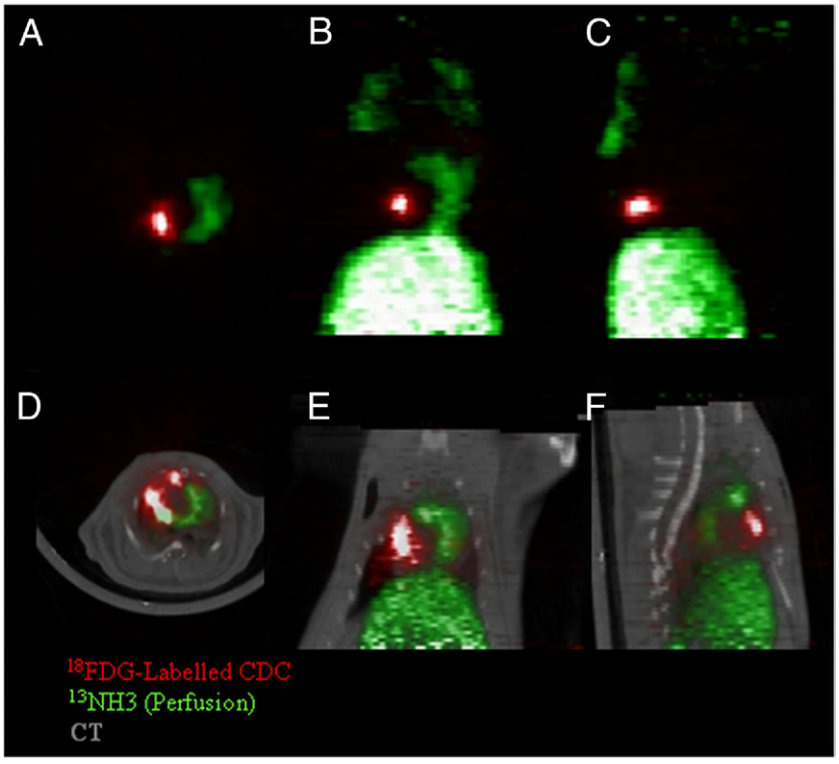

Figure 1 **Detection of ^{18}FDG Labeled Cells Injected in the Myocardium by Micro-PET**

(A) Transverse, **(B)** coronal, **(C)** sagittal image orientation. In a different experiment, fusion of computed tomography (CT) and micro-positron computed tomography (PET) images provides more detailed anatomical information. **(D)** Transverse, **(E)** coronal, **(F)** sagittal image orientation. ^{13}NH3 = ^{13}N-ammonia; ^{18}FDG = [^{18}F]-fluoro-deoxy-glucose.

the site of injection, so as to minimize backwash. In the FG group, retention was significantly increased to 37.5 ± 8.2% ($p < 0.01$ vs. cells in PBS), revealing a dramatic effect of sealing the injection site on cell retention.

Another approach to minimize the effects of cardiac contraction is to slow the heart rate. Adenosine injection lowered the heart rate in all animals of the group and exerted a favorable effect on cell retention (35.4 ± 5.3%, $p < 0.05$ vs. cells in PBS). When IV adenosine was combined with FG use, retention was 39.3 ± 11.6% ($p < 0.01$ vs. cells in PBS). The fact that no significant increase of cell retention over the levels achieved by either technique alone was observed indicates that mean retention rates of approximately 40% are probably the limit in our model. The difference between 40% and the approximately 75% seen in the arrested heart likely reflects the contribution of myocardial perfusion on cell washout from the injection site.

Yet another approach to decrease cardiac contraction is to paralyze the heart locally with a drug that uncouples excitation from contraction. Local injection of BDM along with the CDCs did not result in any improvement of cell retention (14.9 ± 6.9%, p = NS vs. cells in PBS), despite the fact that contractility was transiently suppressed, confirmed by visual inspection at the injection site. The inadequacy of this intervention was probably due to its very transient nature: normal contraction resumed visually a few seconds after BDM injection, reflective of quick washout of the drug from the injection site.

Comparisons of acute cell retention between the different experimental groups are summarized in Figure 2 (1-way analysis of variance, $p < 0.0001$).

Validation of PET quantitative results by qPCR. In 6 animals of the PBS group, retention at 1 h after cell injection, measured by quantitative real-time PCR, was 17.6 ± 11.5%, almost identical to the values obtained by in vivo PET, underscoring the accuracy of quantification with this imaging modality (Fig. 3).

Longer-term engraftment. To determine whether the increase of acute cell retention would have an impact on cell engraftment 3 weeks after cell transplantation, we compared engraftment between the cells in PBS and FG groups, with quantitative real-time PCR. Indeed, in the FG group, cell engraftment was significantly augmented (22.1 ± 18.6% vs. 5.3 ± 3.1%, p = 0.039), indicating that an effective early intervention aimed at improving retention of cells in the infarcted myocardium could have important implications for the sustained presence of these cells in the heart (Fig. 4). In addition, at 3 weeks, green fluorescent protein positive cells

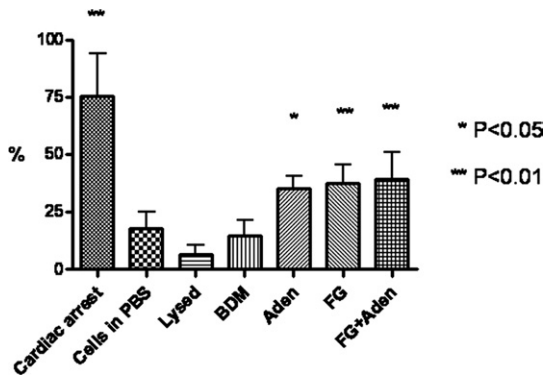

Figure 2 Retention of Intramyocardially Injected Cells at 60 min After Cell Injection, in the Different Experimental Groups

The p values correspond to comparisons between the cells in phosphate buffered saline (PBS) and the intervention groups. Values are reported as mean ± SD. Aden = adenosine; BDM = 2,3-butanedione-2-monoxime; FG = fibrin glue.

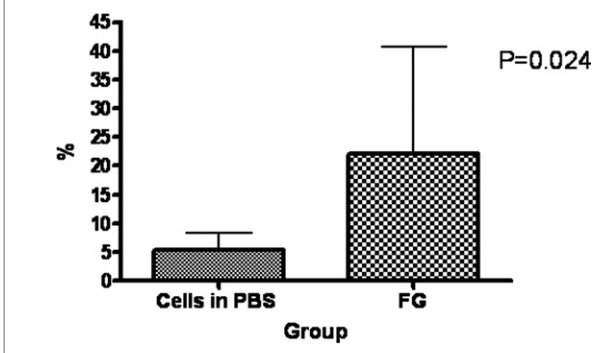

Figure 4 Comparison of Engraftment at 3 Weeks Between the Cells in PBS and FG Groups

Assessment by real-time quantitative polymerase chain reaction, values are reported as mean ± SD. FG = fibrin glue; PBS = phosphate-buffered saline.

were identified by immunocytochemistry in the infarct border zone of 2 of 3 animals of the FG group only, confirming their stable engraftment (Fig. 5).

Functional effect of CDC transplantation. Baseline FAC was 62 ± 10% in the experimental animals. On day 2 after induction of MI, FAC was 39.3 ± 7.1%, 39.1 ± 9.9%, 42.5 ± 9.7%, and 41.6 ± 11% in the PBS only, FG only, cells in PBS, and cells with FG groups, respectively, indicating that infarct sizes were comparable in all groups. In animals that received injection with vehicle only (PBS without or with FG), FAC decreased from day 2 to day 21 after MI (−25.9 ± 23.5% and −7.6 ± 37.2%, respectively). In contrast, in both cells in PBS and FG groups, FAC was significantly improved from day 2 to day 21, when compared with the placebo group of PBS injection only (+7.9 ± 15.6% and 24.3 ± 31%, $p < 0.05$ and $p < 0.01$ vs. PBS only, respectively). Although there was a trend for greater increase in the FG group, in comparison with cells in PBS (indicating that optimizing acute cell retention and engraftment translates to a superior functional benefit, in this model), this did not reach statistical significance, probably because of the large variability (Fig. 6).

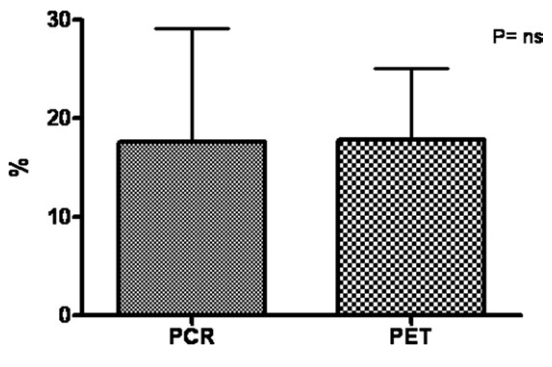

Figure 3 Retention of Intramyocardially Injected Cells 60 min After Cell Injection Measured by In Vivo PET and Real-Time Quantitative PCR

Cells in phosphate buffered saline group-values are reported as mean ± SD. PCR = polymerase chain reaction; PET = positron computed tomography.

Discussion

Acute retention of cells delivered directly into the myocardium is low, compromising the potential of stem cell therapy for myocardial regeneration. In the present study, we applied a safe, nontoxic method for cardiac stem cell

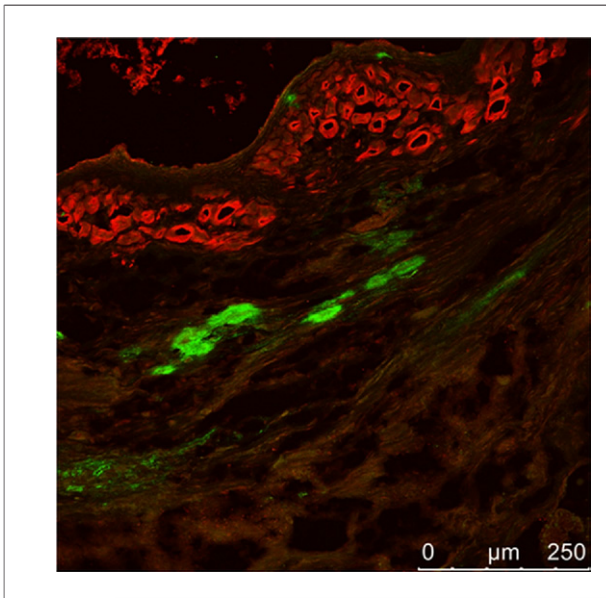

Figure 5 Immunocytochemistry of Frozen Cardiac Sections at 3 Weeks After Cell Injection

The presence of enhanced green fluorescent protein positive cells **(green)** at the infarct border zone (**red**: troponin I), in an animal of the fibrin glue group, was revealed.

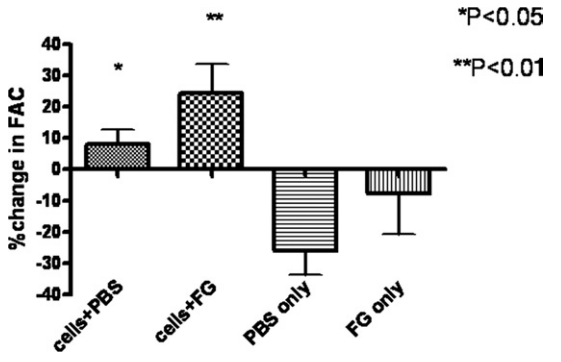

Figure 6 **Percent Change in FAC Between Days 2 and 21 After Myocardial Infarction, in Animals Treated With Cells in PBS, Cells and FG, PBS Only, and FG Only**

One-way analysis of variance, p = 0.002. The p values on the figure correspond to post hoc comparisons between the PBS only and the intervention groups. Values are reported as mean ± SEM. FAC = fractional area change; other abbreviations as in Figures 2 and 3.

radiolabeling; we quantified cell retention by in vivo PET imaging and developed methods for significantly improving the efficiency of intramyocardial injections, with clinically approved compounds.

Many studies in the past acknowledged the problem of low engraftment as one of the main hurdles to a significant functional improvement after stem cell transplantation (4,5,11,26). To address this issue, an easily applicable and potentially translatable method is required for quantitative assessment of cell delivery. Positron emission tomography imaging is particularly attractive for this purpose, because it is noninvasive, sensitive, readily quantifiable, and widely used in clinical practice.

In vivo PET imaging presents a significant advantage over the other available techniques for assessing engraftment, because it allows relative quantification of acute cell retention as a percentage of the net injected activity, thus eliminating errors resulting from cell counting or from residual cells in the dead space of the syringe. In addition, direct radiolabeling presents significant advantages over a reporter gene technique for quantification purposes, because no systemic tracer injections are needed. Thus, the background is minimal, very small numbers of cells can be detected, and the dose of the radiolabel can be kept to very low levels, without sacrificing sensitivity.

Single-photon emission tomography has also been used for short-term tracking of injected cells (7,9,10,12). The inherent lower sensitivity of this modality necessitates the use of relatively large doses of radioactivity to label the cells and obtain adequate images within reasonable time, raising the risks of radiotoxicity (reduced viability or proliferation rates), particularly in sensitive cell types. Several studies have reported substantial toxicity from 111-indium on labeled stem cells (7,12,27). In addition, quantification of single-photon emission tomography images remains challenging, mainly due to the significant confounding effect of scattering (28).

Several groups in the past have used 3-dimensional injectable scaffolds as vehicle for cell implantation and have reported improved results (29). Within this context, fibrin 'glue' seems a particularly attractive option, because it has already been approved for clinical use (30–34). It consists of 2 components, a thrombin/calcium chloride and a fibrinogen/aprotinin solution that are mixed immediately before application. In previous reports, FG was used to facilitate delivery of endothelial cells, skeletal myoblasts, or bone marrow mononuclear cells in the infarcted myocardium (31,32,34). This approach led to an improved functional outcome that was attributed to a higher engraftment rate, although the latter was not documented directly by any quantitative technique. In addition, in all these studies, cells and the 2 components of the glue were mixed, creating an environment that might promote cell clumping or intravascular thrombus formation. In all intramyocardial injections, a fraction of the cells will be either inadvertently injected in the left ventricular cavity and end up in the microcirculation of peripheral organs or will migrate through the cardiac venous system to the right heart and eventually reach the lungs. Fibrin glue solidifies fast after application, enabling the encapsulated cells to create large aggregates within the 3-dimensional scaffold. These aggregates have the potential to embolize, a risk that could preclude clinical application of this material for cell delivery. In addition, the risk of inducing intravascular thrombosis when the thrombin component is injected intravascularly has been recognized in clinical applications, further raising concerns about the safety of the practice of mixing the cells with the compound and injecting it in the myocardium (35,36).

In the present study, we applied the FG exclusively on the epicardium, to either prevent back leak of injected cells due to myocardial contraction or washout by bleeding caused by the injection trauma. We were able to confirm a significant increase in cell retention by PET, and importantly, we showed a benefit in cell engraftment at 3 weeks and a trend toward larger functional benefit. Our modified protocol maintained efficacy while minimizing potential risks, suggesting potential for future clinical applications.

Optimization of cell retention by FG should be confirmed, however, in more clinically relevant models before use in clinical trials of stem cell therapy is attempted. In larger models, the relative volume of the injectate in relation to the myocardial mass is smaller; therefore back leak of cells after intramyocardial injection might be less pronounced, and the need for sealing the injection site might be smaller.

Adenosine was also proven effective in increasing acute CDC retention in the rat model. Although cell injection during adenosine infusion could be easily attempted in the clinical setting, it is difficult to predict the impact of this approach, because heart rates are significantly lower in humans, and injections are less demanding technically. Adenosine, in the doses that can be used safely in clinical

applications, might lead to a significant increase in coronary blood flow, exaggerating the washout of cells from the myocardium. Adenosine has been recently reported to increase the adhesion of endothelial progenitor cells in the coronary microcirculation and increase their cardiac retention, through up-regulation of P-Selectin on endothelial cells (37). This effect is rapid and thus might have played a role in the improved CDC retention we observed with adenosine, although our initial rationale was purely to effect negative chronotropy.

Nevertheless, both FG and adenosine should be tested in large animal models that are more clinically relevant, to determine their true potential. Positron emission tomography seems to be the method of choice to reliably quantify cell retention and to evaluate these and any other cell delivery techniques.

Study limitations. Despite the numerous advantages of PET, the short half-life of most of the available tracers significantly diminishes the potential applications. [^{18}F]-fluoro-deoxy-glucose PET can only be used for tracking the cells within the first few hours after delivery, because this tracer has a half-life of 110 min. However, successful labeling of cells with the PET tracer ^{64}Cu-PTSM has been reported (half-life of 12.7 h), allowing longer-term cell detection (38). In addition, PET availability remains limited to larger centers, although this situation is rapidly changing. Despite these facts, the quality and reproducibility of the results are favorable aspects of this technology for accurate quantification of acute cell retention. Finally, the impact of increased acute retention on long-term engraftment and cardiac function in the adenosine group was not assessed in the present study and should be demonstrated in future experiments.

Conclusions

In vivo PET imaging is an effective, accurate, clinically translatable approach for measurement of acute cell retention after intramyocardial cell injection. It permits assessment of different delivery methods and can contribute to optimization of cellular therapies and functional benefits of transplantation. With PET, we have compared several methods for improving intramyocardial cell delivery and shown that sealing of the epicardial injection site with FG and reduction of ventricular rate by IV adenosine can significantly improve cell retention.

Acknowledgments

The authors would like to thank Dr. R. Smith, PhD, and Dr. D. Davis, MD, for their suggestions concerning histology.

Reprint requests and correspondence: Dr. Eduardo Marbán, Director, The Heart Institute, Cedars Sinai Medical Center, 8700 Beverly Boulevard, 1090 Davis Building, Los Angeles, California 90048. E-mail: Eduardo.Marban@csmc.edu.

REFERENCES

1. Wollert KC, Drexler H. Clinical applications of stem cells for the heart. Circ Res 2005;96:151–63.
2. Murry CE, Reinecke H, Pabon LM. Regeneration gaps: observations on stem cells and cardiac repair. J Am Coll Cardiol 2006;47:1777–85.
3. Segers VF, Lee RT. Stem-cell therapy for cardiac disease. Nature 2008;451:937–42.
4. Fukushima S, Varela-Carver A, Coppen SR, et al. Direct intramyocardial but not intracoronary injection of bone marrow cells induces ventricular arrhythmias in a rat chronic ischemic heart failure model. Circulation 2007;115:2254–61.
5. Robey TE, Saiget MK, Reinecke H, Murry CE. Systems approaches to preventing transplanted cell death in cardiac repair. J Mol Cell Cardiol 2008;45:567–81.
6. Aicher A, Brenner W, Zuhayra M, et al. Assessment of the tissue distribution of transplanted human endothelial progenitor cells by radioactive labeling. Circulation 2003;107:2134–9.
7. Brenner W, Aicher A, Eckey T, et al. 111In-labeled CD34+ hematopoietic progenitor cells in a rat myocardial infarction model. J Nucl Med 2004;45:512–8.
8. Cao F, Lin S, Xie X, et al. In vivo visualization of embryonic stem cell survival, proliferation, and migration after cardiac delivery. Circulation 2006;113:1005–14.
9. Zhou R, Thomas DH, Qiao H, et al. In vivo detection of stem cells grafted in infarcted rat myocardium. J Nucl Med 2005;46:816–22.
10. Goussetis E, Manginas A, Koutelou M, et al. Intracoronary infusion of CD133+ and CD133-CD34+ selected autologous bone marrow progenitor cells in patients with chronic ischemic cardiomyopathy: cell isolation, adherence to the infarcted area, and body distribution. Stem Cells 2006;24:2279–83.
11. Hofmann M, Wollert KC, Meyer GP, et al. Monitoring of bone marrow cell homing into the infarcted human myocardium. Circulation 2005;111:2198–202.
12. Kraitchman DL, Tatsumi M, Gilson WD, et al. Dynamic imaging of allogeneic mesenchymal stem cells trafficking to myocardial infarction. Circulation 2005;112:1451–61.
13. Terrovitis J, Kwok KF, Lautamaki R, et al. Ectopic expression of the sodium-iodide symporter enables imaging of transplanted cardiac stem cells in vivo by single-photon emission computed tomography or positron emission tomography. J Am Coll Cardiol 2008;52:1652–60.
14. Wu JC, Chen IY, Sundaresan G, et al. Molecular imaging of cardiac cell transplantation in living animals using optical bioluminescence and positron emission tomography. Circulation 2003;108:1302–5.
15. Bengel FM, Schachinger V, Dimmeler S. Cell-based therapies and imaging in cardiology. Eur J Nucl Med Mol Imaging 2005;32 Suppl 2:S404–16.
16. Frangioni JV, Hajjar RJ. In vivo tracking of stem cells for clinical trials in cardiovascular disease. Circulation 2004;110:3378–83.
17. Messina E, De Angelis L, Frati G, et al. Isolation and expansion of adult cardiac stem cells from human and murine heart. Circ Res 2004;95:911–21.
18. Smith RR, Barile L, Cho HC, et al. Regenerative potential of cardiosphere-derived cells expanded from percutaneous endomyocardial biopsy specimens. Circulation 2007;115:896–908.
19. Hayashi M, Martinez OM, Krams SM, Burns W, Esquivel CO. Characterization of allograft rejection in an experimental model of small intestinal transplantation. J Gastrointest Surg 1998;2:325–32.
20. Swanger SA, Neuhuber B, Himes BT, Bakshi A, Fischer I. Analysis of allogeneic and syngeneic bone marrow stromal cell graft survival in the spinal cord. Cell Transplant 2005;14:775–86.
21. Backx PH, Gao WD, Azan-Backx MD, Marban E. Mechanism of force inhibition by 2,3-butanedione monoxime in rat cardiac muscle: roles of [Ca2+]i and cross-bridge kinetics. J Physiol 1994;476:487–500.
22. Smith TL, Coleman TG, Stanek KA, Murphy WR. Hemodynamic monitoring for 24 h in unanesthetized rats. Am J Physiol 1987;253:H1335–41.
23. Wang Y, Seidel J, Tsui BM, Vaquero JJ, Pomper MG. Performance evaluation of the GE healthcare eXplore VISTA dual-ring small-animal PET scanner. J Nucl Med 2006;47:1891–900.
24. Chow PL, Rannou FR, Chatziioannou AF. Attenuation correction for small animal PET tomographs. Phys Med Biol 2005;50:1837–50.

25. Loening AM, Gambhir SS. AMIDE: a free software tool for multimodality medical image analysis. Mol Imaging 2003;2:131–7.
26. Laflamme MA, Chen KY, Naumova AV, et al. Cardiomyocytes derived from human embryonic stem cells in pro-survival factors enhance function of infarcted rat hearts. Nat Biotechnol 2007;25:1015–24.
27. Jin Y, Kong H, Stodilka RZ, et al. Determining the minimum number of detectable cardiac-transplanted 111In-tropolone-labelled bone-marrow-derived mesenchymal stem cells by SPECT. Phys Med Biol 2005;50:4445–55.
28. Zaidi H, Koral KF. Scatter modelling and compensation in emission tomography. Eur J Nucl Med Mol Imaging 2004;31:761–82.
29. Yang Y, El Haj AJ. Biodegradable scaffolds—delivery systems for cell therapies. Expert Opin Biol Ther 2006;6:485–98.
30. Ahmed TA, Dare EV, Hincke M. Fibrin: a versatile scaffold for tissue engineering applications. Tissue Eng Part B Rev 2008;14:199–215.
31. Chekanov V, Akhtar M, Tchekanov G, et al. Transplantation of autologous endothelial cells induces angiogenesis. Pacing Clin Electrophysiol 2003;26:496–9.
32. Christman KL, Fok HH, Sievers RE, Fang Q, Lee RJ. Fibrin glue alone and skeletal myoblasts in a fibrin scaffold preserve cardiac function after myocardial infarction. Tissue Eng 2004;10:403–9.
33. Christman KL, Vardanian AJ, Fang Q, Sievers RE, Fok HH, Lee RJ. Injectable fibrin scaffold improves cell transplant survival, reduces infarct expansion, and induces neovasculature formation in ischemic myocardium. J Am Coll Cardiol 2004;44:654–60.
34. Ryu JH, Kim IK, Cho SW, et al. Implantation of bone marrow mononuclear cells using injectable fibrin matrix enhances neovascularization in infarcted myocardium. Biomaterials 2005;26:319–26.
35. Goerler H, Oppelt P, Abel U, Haverich A. Safety of the use of Tissucol Duo S in cardiovascular surgery: retrospective analysis of 2149 patients after coronary artery bypass grafting. Eur J Cardiothorac Surg 2007;32:560–6.
36. Lamm P, Adelhard K, Juchem G, et al. Fibrin glue in coronary artery bypass grafting operations: casting out the devil with Beelzebub? Eur J Cardiothorac Surg 2007;32:567–72.
37. Ryzhov S, Solenkova NV, Goldstein AE, et al. Adenosine receptor-mediated adhesion of endothelial progenitors to cardiac microvascular endothelial cells. Circ Res 2008;102:356–63.
38. Adonai N, Nguyen KN, Walsh J, et al. Ex vivo cell labeling with 64Cu-pyruvaldehyde-bis(N4-methylthiosemicarbazone) for imaging cell trafficking in mice with positron-emission tomography. Proc Natl Acad Sci U S A 2002;99:3030–5.

Key Words: adenosine ■ cardiac stem cells ■ fibrin glue ■ PET.

APPENDIX

For supplementary data regarding the animal model, imaging, qPCR and histology protocols, please see the online version of this article.